

# Three-directional Box-Splines: Characterization and Efficient Evaluation

Laurent Condat, *Student Member, IEEE*, and Dimitri Van De Ville, *Member, IEEE*

**Abstract**—We propose a new characterization of three-directional box-splines, which are well adapted for interpolation and approximation on hexagonal lattices. Inspired by a construction already applied with success for exponential splines [1] and hex-splines [2], we characterize a box-spline as a convolution of a generating function, that is a Green function of the spline's associated differential operator, and a discrete filter that plays the role of a localization operator. This process leads to an elegant analytical expression of three-directional box-splines. It also brings along a particularly efficient implementation.

**Index Terms**—Box-splines, hexagonal sampling, three-directional mesh, interpolation, approximation.

## I. INTRODUCTION

THE representation of a digital signal by means of a discrete/continuous model is essential for common tasks such as interpolation and resampling. For images and other two-dimensional (2-D) data, polynomial spline models based on B-splines are particularly popular, mainly due to their simplicity and excellent approximation capabilities [3].

For image data sampled on the traditional Cartesian lattice, separable B-splines can be obtained in a straightforward way using tensor products of one-dimensional (1-D) B-splines. However, in the case of sampling on a hexagonal lattice (a.k.a. three-directional mesh) separable B-splines are unable to exploit the highly praised isotropy and twelve-fold symmetry of this sampling scheme [4], [5]. *Box-splines* are a multi-dimensional extension of 1-D splines [6] that have found practical applications in geometric modelling, multiscale representation, and many other fields [7]. Among the large box-spline family, three-directional (non-separable) box-splines are particularly suitable for hexagonal lattices. They have been successfully applied in numerous problems where hexagonally sampled data are handled [8], [9].

Early algorithms to evaluate box-spline surfaces were very memory consuming and only resulted into an approximation of the surface within a given tolerance [10]–[12]. Later, more efficient methods were proposed based on the recursive properties of box-splines [13]–[16]. Here, we propose a new characterization of three-directional box-splines that provides us with a closed analytical formula, as well as an efficient implementation scheme. To this aim, we derive an explicit form of the generating function, which is the Green function

of a three-directional differential operator associated with box-splines. Then, the box-spline can be expressed as the convolution of the generating function with a discrete filter, which plays the role of a localization operator. A similar construction was already applied on the Cartesian lattice to generalized polynomial splines (i.e., exponential splines and L-splines [1]) and to the design of another family of splines on the hexagonal lattice (i.e., hex-splines [2]).

## II. BOX-SPLINES ON THE HEXAGONAL LATTICE

### A. Mathematical preliminaries

A 2-D lattice is a set of points of the plane, characterized by two linearly independent vectors  $\mathbf{v}_1$  and  $\mathbf{v}_2$  grouped in a matrix  $\mathbf{R} = [\mathbf{v}_1 \ \mathbf{v}_2]$ , such that the lattice sites are the locations  $\mathbf{R}\mathbf{k}$  for every  $\mathbf{k} \in \mathbb{Z}^{2 \times 1}$ . Within this letter, we define the vectors  $\mathbf{e}_1 = [1 \ 0]^T$ ,  $\mathbf{e}_2 = [0 \ 1]^T$ , and those shown in Fig. 1 as

$$\mathbf{r}_1 = \begin{bmatrix} 1/2 \\ -\sqrt{3}/2 \end{bmatrix}, \quad \mathbf{r}_2 = \begin{bmatrix} 1/2 \\ \sqrt{3}/2 \end{bmatrix}, \quad \mathbf{r}_3 = \begin{bmatrix} 1 \\ 0 \end{bmatrix}. \quad (1)$$

The Cartesian lattice is then obtained for  $\mathbf{R} = [\mathbf{e}_1 \ \mathbf{e}_2]$ , and the regular hexagonal lattice, as in Fig. 1, for  $\mathbf{R} = [\mathbf{r}_1 \ \mathbf{r}_2]$ .

Bivariate functions are equivalently denoted as  $f(x_1, x_2)$ ,  $x_1, x_2 \in \mathbb{R}$ , or  $f(\mathbf{x})$ , where  $\mathbf{x} = [x_1 \ x_2]^T$  is interpreted as a vector in  $\mathbb{R}^2$ . The Fourier transform of a function  $f(\mathbf{x}) \in L_2(\mathbb{R}^2)$  is defined as  $\hat{f}(\boldsymbol{\omega}) = \int_{\mathbb{R}^2} f(\mathbf{x}) \exp(-j\langle \boldsymbol{\omega}, \mathbf{x} \rangle) d\mathbf{x}$ , where  $\langle \boldsymbol{\omega}, \mathbf{x} \rangle = \boldsymbol{\omega}^T \mathbf{x}$  is the usual inner product of vectors.

A 2-D discrete signal is denoted as  $s[\mathbf{k}] = s[k_1, k_2]$ ,  $k_1, k_2 \in \mathbb{Z}$ . Its representation in the continuous domain, associated with the lattice sites  $\mathbf{R}\mathbf{k}$ , is a weighted Dirac comb:  $s(\mathbf{x}) = \sum_{\mathbf{k} \in \mathbb{Z}^2} s[\mathbf{k}] \delta(\mathbf{x} - \mathbf{R}\mathbf{k})$ . Consequently, its Fourier transform is defined accordingly as  $\hat{s}(\boldsymbol{\omega}) = \sum_{\mathbf{k} \in \mathbb{Z}^2} s[\mathbf{k}] \exp(-j\langle \boldsymbol{\omega}, \mathbf{R}\mathbf{k} \rangle)$ . For  $\mathbf{z} = \exp(-j\mathbf{R}^T \boldsymbol{\omega})$ , we get the  $\mathcal{Z}$ -transform of  $s$  as  $S(\mathbf{z}) = \sum_{\mathbf{k} \in \mathbb{Z}^2} s[\mathbf{k}] \mathbf{z}^{-\mathbf{k}}$  ( $\mathbf{z}^{-\mathbf{k}}$  means  $z_1^{-k_1} z_2^{-k_2}$ ). Continuous and discrete convolutions are denoted by  $*$ .

### B. Definition

A 2-D box-spline model defined on a lattice  $\mathbf{R}$  has the form

$$f(\mathbf{x}) = \sum_{\mathbf{k} \in \mathbb{Z}^2} c[\mathbf{k}] \varphi_{\Xi}(\mathbf{x} - \mathbf{R}\mathbf{k}), \quad \mathbf{x} \in \mathbb{R}^2, \quad (2)$$

where  $c[\mathbf{k}]$  are the box-spline coefficients that are weights for the box-spline basis functions  $\varphi_{\Xi}(\mathbf{x})$ , placed on every lattice site. They can be computed to ensure a desired property, typically that  $f$  interpolates a discrete available signal  $s$  (i.e.  $f(\mathbf{R}\mathbf{k}) = s[\mathbf{k}]$  for every  $\mathbf{k}$ ). The box-spline  $\varphi_{\Xi}(\mathbf{x})$  depends on a concatenated matrix of  $N$  vectors  $\Xi = [\mathbf{v}_1 \ \cdots \ \mathbf{v}_N]$

The first author is with the Laboratory of Images and Signals (LIS), Institut National Polytechnique de Grenoble (INPG), 38031 Grenoble, France (e-mail: laurent.condat@lis.inpg.fr). The second author is with the Biomedical Imaging Group (BIG), École Polytechnique Fédérale de Lausanne (EPFL), CH-1015 Lausanne, Switzerland (e-mail: dimitri.vandeville@epfl.ch).

This work was initiated during the first author's visit at BIG, supported by Région Rhône-Alpes (EURODOC grant).

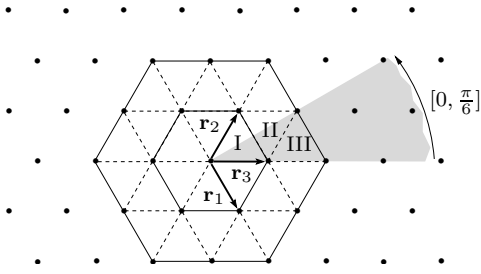


Fig. 1. The hexagonal lattice is generated using integer combinations of the vectors  $\mathbf{r}_1$ ,  $\mathbf{r}_2$ ,  $\mathbf{r}_3$ . The hexagonal support of the first two box-splines  $\chi^1(\mathbf{x})$  and  $\chi^2(\mathbf{x})$  has been indicated. Box-splines are polynomial inside each triangle. Using the twelve-fold symmetry,  $\chi^1$  and  $\chi^2$  have only to be known in the triangles I, II, III, that intersect the sector  $[0, \pi/6]$ .

( $N \geq 2$ ), and can be defined as follows [6]: if  $\Xi = [\mathbf{v}_1 \ \mathbf{v}_2]$ , then

$$\varphi_{[\mathbf{v}_1 \ \mathbf{v}_2]}(\mathbf{x}) = \begin{cases} 1/|\det(\Xi)|, & \text{if } \Xi^{-1}\mathbf{x} \in [0, 1)^2, \\ 0, & \text{otherwise,} \end{cases} \quad (3)$$

and inductively,  $\varphi_{\Xi \cup [\mathbf{v}]}(\mathbf{x}) = \int_0^1 \varphi_{\Xi}(\mathbf{x} - t\mathbf{v}) dt$ .

Therefore, we have the normalization  $\int_{\mathbb{R}^2} \varphi_{\Xi} = 1$  and the convolution property  $\varphi_{\Xi_1 \cup \Xi_2} = \varphi_{\Xi_1} * \varphi_{\Xi_2}$ .

On a hexagonal lattice, box-splines can be constructed using the three vectors  $\mathbf{r}_1$ ,  $\mathbf{r}_2$ ,  $-\mathbf{r}_3$ . In particular, we define the so-called Courant element [6] as  $\chi^1 = \frac{\sqrt{3}}{2} \varphi_{[\mathbf{r}_1 \ \mathbf{r}_2 \ -\mathbf{r}_3]}$ , where we have changed the normalization towards the density of the lattice, i.e.,  $|\det \mathbf{R}| = \frac{\sqrt{3}}{2}$ . Further on, higher orders are obtained as  $\chi^n = \frac{2}{\sqrt{3}} \chi^{n-1} * \chi^1$ ,  $n > 1$ . Their expression in the Fourier domain is

$$\hat{\chi}^n(\boldsymbol{\omega}) = \frac{\sqrt{3}}{2} \left( \frac{\exp(j\langle \boldsymbol{\omega}, \mathbf{r}_3 \rangle) \prod_{i=1}^3 1 - \exp(-j\langle \boldsymbol{\omega}, \mathbf{r}_i \rangle)}{(j\langle \boldsymbol{\omega}, \mathbf{r}_1 \rangle)(j\langle \boldsymbol{\omega}, \mathbf{r}_2 \rangle)(j\langle \boldsymbol{\omega}, \mathbf{r}_3 \rangle)} \right)^n \quad (4)$$

$$= \frac{\sqrt{3}}{2} \prod_{i=1}^3 \text{sinc}(\langle \boldsymbol{\omega}, \mathbf{r}_i \rangle / 2)^n. \quad (5)$$

where  $\text{sinc}(x) = \sin(x)/x$ . The box-splines  $\chi^n(\mathbf{x})$  have several attractive properties such as an hexagonal compact support and twelve-fold symmetry, as illustrated in Figs 1 and 2. In the next section, we provide closed analytical formulas for these box-splines in the spatial domain.

### III. DIFFERENTIAL CHARACTERIZATION OF BOX-SPLINES

#### A. B-spline refresher

In the 1-D case, a polynomial spline  $f(x)$  for uniformly sampled data can be expressed similarly to (2) as  $f(x) = \sum_{k \in \mathbb{Z}} c[k] \beta^n(x - k)$ .  $\beta^n$  is the causal B-spline of degree  $n \in \mathbb{N}$ , which is defined in the spatial domain as<sup>1</sup>

$$\beta^n(x) = \Delta^{n+1} * (x)_+^n / n!. \quad (6)$$

We identify  $\Delta^n$  as the  $n^{\text{th}}$  iterate of the finite difference filter, which is usually expressed in the  $\mathcal{Z}$ -domain as  $\Delta^n(z) = (1 - z^{-1})^n$ . Further on, we have the one-sided power function

<sup>1</sup>Note that the 1-D B-spline can also be obtained recursively as  $\beta^n = \beta^{n-1} * \beta^0$ ,  $n > 0$ , with  $\beta^0 = \mathbb{1}_{[0,1]}$  the indicator function of the unit interval.

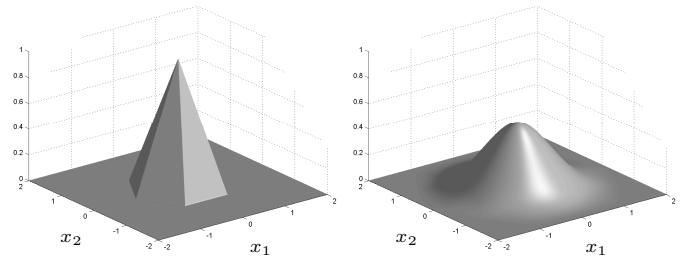


Fig. 2. First two box-splines  $\chi^1(\mathbf{x})$  (left) and  $\chi^2(\mathbf{x})$  (right).

$(x)_+^n = \{x^n, \text{ for } x > 0; 0, \text{ otherwise}\}$ . The filtering process acts as a localization operator on the power function; i.e.,  $\beta^n$  has a finite support. The term  $(x)_+^n / n!$  is also called the generating function and it corresponds to the (causal) Green function of the differential operator  $L^n = d^n/dx^n$ ; i.e., the function  $\rho(x)$  such that  $L^n \{\rho\}(x) = \delta(x)$ . This means that a polynomial spline of degree  $n$ , when differentiated  $n + 1$  times, is a weighted Dirac comb.

On the 2-D Cartesian lattice, we can easily use tensor-product B-splines:  $\beta^n(\mathbf{x}) = \beta^n(x_1)\beta^n(x_2)$ . Then, the associated differential operator is

$$L^n = \frac{\partial^{2n}}{\partial x_1^n \partial x_2^n} = D_{\mathbf{e}_1}^n D_{\mathbf{e}_2}^n \xrightarrow{\mathcal{F}} (j\langle \boldsymbol{\omega}, \mathbf{e}_1 \rangle)^n (j\langle \boldsymbol{\omega}, \mathbf{e}_2 \rangle)^n, \quad (7)$$

where  $D_{\mathbf{v}} f(\mathbf{x}) = \lim_{t \rightarrow 0} (f(\mathbf{x} + t\mathbf{v}) - f(\mathbf{x})) / t$ . In that case, the (separable) generating function is  $(\mathbf{x})_+^n / (n!)^2 = (x_1)_+^n (x_2)_+^n / (n!)^2$  and the corresponding localization operator  $\Delta^n(\mathbf{z}) = \Delta^n(z_1)\Delta^n(z_2)$ .

#### B. From differential operators to generating functions

Inspired by the B-spline construction using Green functions, we propose an extension for the box-splines on the hexagonal lattice. For this purpose, we introduce the three-directional differential operator  $L^n = \frac{2}{\sqrt{3}} D_{\mathbf{r}_1}^n D_{\mathbf{r}_2}^n D_{\mathbf{r}_3}^n$ ,  $n \geq 1$ . Its Fourier transform, in the sense of the distributions, is

$$\hat{L}^n(\boldsymbol{\omega}) = \frac{2}{\sqrt{3}} (j\langle \boldsymbol{\omega}, \mathbf{r}_1 \rangle)^n (j\langle \boldsymbol{\omega}, \mathbf{r}_2 \rangle)^n (j\langle \boldsymbol{\omega}, \mathbf{r}_3 \rangle)^n. \quad (8)$$

PROPOSITION: A Green function  $\rho^n(\mathbf{x})$  of the operator  $L^n$ ,  $n \geq 1$ , is given by

$$\rho^n(\mathbf{x}) = \sum_{i=0}^{n-1} \binom{n-1+i}{i} \mu^{n-1-i, 2n-1+i}(\mathbf{x}), \quad (9)$$

where

$$\mu^{n_1, n_2}(x_1, x_2) = \frac{1}{n_1! n_2!} \left( \frac{2|x_2|}{\sqrt{3}} \right)^{n_1} \left( x_1 - \frac{|x_2|}{\sqrt{3}} \right)_+^{n_2}. \quad (10)$$

The proof is given in Appendix I. Notice that the functions  $\mu^{n_1, n_2}$  and  $\rho^n$  all have the same wedge-like support; they are causal in  $x_1$  and symmetric in  $x_2$ , as illustrated in Fig. 3.

#### C. From generating functions to box-splines

In the Fourier domain, the generating function  $\rho^n$  corresponds to  $\hat{\chi}^n$  without its numerator in (4). The remaining term can be identified by introducing the discrete filter

$$\Delta(\mathbf{z}) = (1 - z_1^{-1})(1 - z_2^{-1})(z_1 z_2 - 1). \quad (11)$$

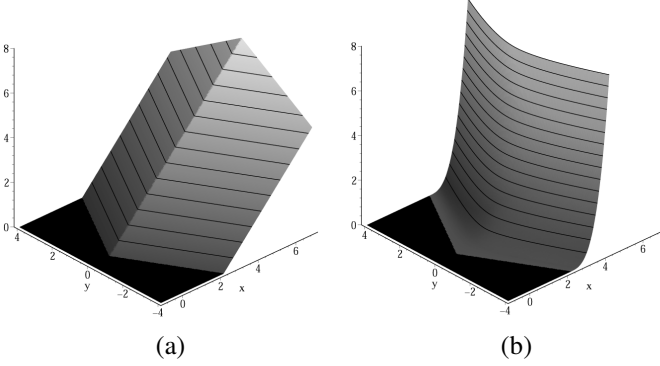


Fig. 3. The Green functions  $\rho^1 = \mu^{0,1}$  in (a), and  $\rho^2 = \mu^{1,3} + 2\mu^{0,4}$  in (b), which serve to generate the box-splines  $\chi^1$  and  $\chi^2$ .

Using the property  $\mathbf{r}_3 = \mathbf{r}_1 + \mathbf{r}_2$ , we find that  $\hat{\Delta}^n(\omega) = \Delta(\exp(j\langle\omega, \mathbf{r}_1\rangle), \exp(j\langle\omega, \mathbf{r}_2\rangle))^n$  is exactly the numerator of (4). We can explicitly find the filter coefficients of  $\Delta^n$  by expanding the  $n$ -th power of the  $\mathcal{Z}$ -transform of (11). By collecting the coefficient in front of the term  $z_1^{-k_1} z_2^{-k_2}$ , we get for every  $k_1, k_2 \in \mathbb{Z}$ :

$$\Delta^n[k_1, k_2] = \sum_{i=\max(k_1, k_2, 0)}^{\min(n+k_1, n+k_2, n)} (-1)^{k_1+k_2+i} \binom{n}{i-k_1} \binom{n}{i-k_2} \binom{n}{i}. \quad (12)$$

By arranging the  $\Delta^n[\mathbf{k}]$  at the lattice sites  $\mathbf{R}\mathbf{k} = k_1\mathbf{r}_1 + k_2\mathbf{r}_2$ , we can represent the first two localization filters as:

$$\Delta = \begin{pmatrix} 1 & -2 & 1 \\ -1 & 1 & 0 & -1 \\ -1 & 1 & 1 & -2 \end{pmatrix}, \quad \Delta^2 = \begin{pmatrix} 2 & 2 & 2 & -2 \\ 1 & 2 & -6 & 2 & 1 \\ -2 & 2 & 2 & -2 \\ 1 & -2 & 1 \end{pmatrix}. \quad (13)$$

Putting together (11) and (8) with the fact that  $\hat{L}^n(\omega)\hat{\rho}^n(\omega) = 1$ , we find that  $\hat{\chi}^n(\omega) = \hat{\Delta}^n(\omega)\hat{\rho}^n(\omega)$ . Therefore, we obtain the characterization:

$$\chi^n(\mathbf{x}) = \Delta^n * \rho^n(\mathbf{x}) = \sum_{\mathbf{k} \in \mathbb{Z}^2} \Delta^n[\mathbf{k}] \rho^n(\mathbf{x} - \mathbf{R}\mathbf{k}). \quad (14)$$

The complete analytical expression of  $\chi^n(\mathbf{x})$ ,  $n \geq 1$ , can then be written as  $\chi^n(x_1, x_2) =$

$$\sum_{k_1, k_2 = -n}^n \sum_{i=\max(k_1, k_2, 0)}^{\min(n+k_1, n+k_2, n)} (-1)^{k_1+k_2+i} \binom{n}{i-k_1} \binom{n}{i-k_2} \binom{n}{i} \sum_{d=0}^{n-1} \binom{n-1+d}{d} \frac{1}{(2n-1+d)!(n-1-d)!} \left| \frac{2x_2}{\sqrt{3}} + k_1 - k_2 \right|^{n-1-d} \left( x_1 - \frac{k_1+k_2}{2} - \left| \frac{x_2}{\sqrt{3}} + \frac{k_1-k_2}{2} \right| \right)_+^{2n-1+d}. \quad (15)$$

#### IV. IMPLEMENTATION ISSUES

##### A. The generic case

Equation (15) provides us with an efficient way to evaluate at any point  $\mathbf{x}$ , any three-directional box-spline  $\chi^n$ . Notice that the power functions grow rapidly, as shown in Fig. 3, which

could lead to problems of numerical stability. A simple remedy consists of evaluating  $\chi^n$  only for  $x_1 \leq 0$ , which exploits the causality of  $\rho^n$  in  $x_1$  and the symmetry  $\chi^n(x_1, x_2) = \chi^n(-x_1, x_2)$ . The following Matlab code performs box-spline evaluations for a list of points  $(\mathbf{x}[\mathbf{m}], \mathbf{y}[\mathbf{m}])$ , indexed by  $\mathbf{m}$ . The twelve-fold symmetry is used to fold coordinates into the sector  $[5\pi/6, \pi]$ , where the number of evaluations of the power functions is minimal. We use the coordinates  $(u, v)$  in the basis  $(\mathbf{r}_1, \mathbf{r}_2)$ , instead of the coordinates  $(x, y)$  in the canonical basis  $(\mathbf{e}_1, \mathbf{e}_2)$ .  $\text{nchoosek}(n, k)$  gives the binomial coefficient  $\binom{n}{k}$ .

```
function val=boxspline(x,y,n)
x=-abs(x); y=abs(y);
u=x-y/sqrt(3); v=x+y/sqrt(3);
id=find(v>0); v(id)=-v(id); u(id)=u(id)+v(id);
id=find(v>u/2); v(id)=u(id)-v(id);
val=zeros(size(x));
for K=-n:ceil(max(max(u)))-1,
    for L=-n:ceil(max(max(v)))-1,
        for i=0:min(n+K,n+L),
            coeff=(-1)^(K+L+i)*nchoosek(n,i-K)*...
                nchoosek(n,i-L)*nchoosek(n,i);
            for d=0:n-1,
                aux=abs(v-L-u+K);
                aux2=(u-K+v-L-aux)/2;
                aux2(find(aux2<0))=0;
                val=val+coeff*nchoosek(n-1+d,d)/...
                    factorial(2*n-1+d)/factorial(n-1-d)*...
                    aux.^(n-1-d).*aux2.^(2*n-1+d);
            end, end, end, end
```

This code was used to generate the plots in Fig. 2. The computational complexity is polynomial in  $n$ , compared to exponential for recursive methods in the literature [13]–[16]. For example, the evaluation  $\text{boxspline}(1, 1, 3)$  took 0.002s, while 47s were required for the same operation using the Matlab code proposed in [15] (that can evaluate any box-spline, not just the three-directional ones).

##### B. Further optimization for fixed $n$

For evaluating a box-spline  $\chi^n$  of fixed  $n$ , an attractive hybrid analytical/numerical implementation consists in determining the polynomial form  $p(\mathbf{x})$  inside each triangle of the three-directional mesh. This polynomial, which is obtained by the sums of (15), can be precomputed, stored, and only evaluated at the end. The following code in C-language for  $\chi^2$  may serve as a template: coordinates are first folded in the sector  $[0, \pi/2]$ , then in  $[0, \pi/3]$  and finally in  $[0, \pi/6]$ . This is done conveniently with the coordinates  $(u, v)$ . The coordinates  $(g = u - v/2, v)$  in the orthogonal basis  $(\mathbf{r}_1, (\mathbf{r}_2 + \mathbf{r}_3)/2)$  are the most appropriate for having short polynomials with rational coefficients in each triangle.

```
float boxspline2(float x, float y) {
    float u=fabs(x)-fabs(y)/sqrt(3.0);
    float v=fabs(x)+fabs(y)/sqrt(3.0);
    if (u<0) { u=-u; v=v+u; } /*symmetry % r2*/
    if (2*u<v) u=v-u; /*symmetry % r2+r3*/
    float g=u-v/2.0;
    if (v>2.0) return 0.0; /*outside the support*/
    if (v<1.0) return 0.5+((5/3.0-v/8.0)*v-3)*v*v/4.0+
        ((1-v/4.0)*v+g*g/6.0-1)*g*g; /*triangle I*/
    if (u>1.0) return (v-2)*(v-2)*(v-2)*(g-1)/6.0;
    return 5/6.0+((1+(1/3.0-v/8.0)*v)*v/4.0-1)*v+
        ((1-v/4.0)*v+g*g/6.0-1)*g*g; /*triangle II*/
}
```

## V. CONCLUSION

We proposed a new characterization of the three-directional box-splines, based on a Green function of the differential operator adapted to the hexagonal lattice. Together with a finite difference filter that acts as a localization operator on the generating function, this provides us with new explicit analytical formulas for the three-directional box-splines. This characterization also leads to particularly easy and efficient implementations. We provided the Matlab source code for the generic case and a further optimized C-code for the case  $n = 2$ . The latter one could be particularly interesting for high-quality visualization of data sampled on a hexagonal lattice.

Finally, we note that these box-splines can be expressed on any lattice with matrix  $\mathbf{R}'$ , and not only on the hexagonal one, by the simple change of basis  $\chi^n(\mathbf{R}\mathbf{R}'^{-1}\mathbf{x})$ .

## APPENDIX I PROOF OF THE PROPOSITION

We verify whether  $\rho^n$  of (9) is a Green function of  $L^n$ ; i.e., we need  $L^n\{\rho^n\}(\mathbf{x}) = \delta(\mathbf{x})$ . First, we introduce the vectors

$$\mathbf{r}_1^\perp = \begin{bmatrix} 1 \\ 1/\sqrt{3} \end{bmatrix}, \quad \mathbf{r}_2^\perp = \begin{bmatrix} 1 \\ -1/\sqrt{3} \end{bmatrix}, \quad \mathbf{r}_3^\perp = \begin{bmatrix} 0 \\ 2/\sqrt{3} \end{bmatrix}, \quad (16)$$

which allow us to express the dual bases of  $(\mathbf{r}_2, \mathbf{r}_3)$  and  $(\mathbf{r}_1, \mathbf{r}_3)$  as  $(\mathbf{r}_3^\perp, \mathbf{r}_2^\perp)$  and  $(-\mathbf{r}_3^\perp, \mathbf{r}_1^\perp)$ , respectively. For example, the coordinates of  $\mathbf{x}$  in  $(\mathbf{r}_2, \mathbf{r}_3)$  are  $(\langle \mathbf{x}, \mathbf{r}_3^\perp \rangle, \langle \mathbf{x}, \mathbf{r}_2^\perp \rangle)$ .

We now derive the Fourier expression of  $\mu^{n_1, n_2}$ , which we first rewrite as

$$\begin{aligned} \mu^{n_1, n_2}(x_1, x_2) &= (x_2)_+^0 \mu^{n_1, n_2}(x_1, x_2) + (-x_2)_+^0 \mu^{n_1, n_2}(x_1, x_2) \\ &= (\langle \mathbf{x}, \mathbf{r}_3^\perp \rangle)_+^{n_1} (\langle \mathbf{x}, \mathbf{r}_2^\perp \rangle)_+^{n_2} + (\langle \mathbf{x}, -\mathbf{r}_3^\perp \rangle)_+^{n_1} (\langle \mathbf{x}, \mathbf{r}_1^\perp \rangle)_+^{n_2}. \end{aligned}$$

From distribution theory, we know the Fourier transform of the one-sided power function

$$(x)_+^n \xleftrightarrow{\mathcal{F}} \frac{n!}{(j\omega)^{n+1}} + \mathcal{D}(\omega), \quad (17)$$

where  $\mathcal{D}$  is essentially the  $n$ -th derivative of Dirac. This term can be omitted since it does not have any influence when applying a differential operator of order  $n$  (continuous or discrete) to  $(x)_+^n$ , also see [2, Appendix C].

Hence, using a tensor product and a change of basis from  $(\mathbf{e}_1, \mathbf{e}_2)$  to  $(\mathbf{r}_2, \mathbf{r}_3)$  (with Jacobian  $|\det[\mathbf{r}_2 \ \mathbf{r}_3]| = \frac{\sqrt{3}}{2}$ ), we get

$$(x_2)_+^0 \mu^{n_1, n_2} \xleftrightarrow{\mathcal{F}} \frac{\sqrt{3}/2}{(j\langle \omega, \mathbf{r}_2 \rangle)^{n_1+1} (j\langle \omega, \mathbf{r}_3 \rangle)^{n_2+1}}. \quad (18)$$

Similarly, the Fourier transform of  $(-x_2)_+^0 \mu^{n_1, n_2}$  is obtained by replacing  $\mathbf{r}_2$  by  $\mathbf{r}_1$  in (18).

We now define the functions  $\gamma^{n_1, n_2, n_3}$ , for any integers  $n_1, n_2, n_3$  as

$$\gamma^{n_1, n_2, n_3} \xleftrightarrow{\mathcal{F}} \frac{\sqrt{3}/2}{(j\langle \omega, \mathbf{r}_1 \rangle)^{n_1} (j\langle \omega, \mathbf{r}_2 \rangle)^{n_2} (j\langle \omega, \mathbf{r}_3 \rangle)^{n_3}}. \quad (19)$$

We recognize  $\rho^n = \gamma^{n, n, n}$ ,  $n \geq 1$ . Using the property  $\mathbf{r}_3 = \mathbf{r}_1 + \mathbf{r}_2$ , we can further obtain the following recurrence relation,

for  $n_1 \geq 1, n_2 \geq 1, n_3 \geq 0$ :

$$\gamma^{n_1, n_2, n_3} = \gamma^{n_1-1, n_2, n_3+1} + \gamma^{n_1, n_2-1, n_3+1}. \quad (20)$$

By recurrence on  $n_1 + n_2$ , we can also show that

$$\begin{aligned} \gamma^{n_1, n_2, n_3} &= \sum_{i=0}^{n_1-1} \binom{n_2-1+i}{i} \gamma^{n_1-i, 0, n_2+n_3+i} \\ &\quad + \sum_{i=0}^{n_2-1} \binom{n_1-1+i}{i} \gamma^{0, n_2-i, n_1+n_3+i}. \end{aligned} \quad (21)$$

In the case of  $\rho^n$ , we have

$$\rho^n = \sum_{i=0}^{n-1} \binom{n-1+i}{i} (\gamma^{n-i, 0, 2n+i} + \gamma^{0, n-i, 2n+i}). \quad (22)$$

Finally, we identify the function  $\mu^{n_1, n_2}$  as

$$\mu^{n_1, n_2} = \gamma^{0, n_1+1, n_2+1} + \gamma^{n_1+1, 0, n_2+1}, \quad (23)$$

which results into (9).

## REFERENCES

- [1] M. Unser and T. Blu, "Cardinal exponential splines: Part I—Theory and filtering algorithms," *IEEE Trans. Signal Processing*, vol. 53, no. 4, pp. 1425–1438, Apr. 2005.
- [2] D. Van De Ville, T. Blu, M. Unser, W. Philips, I. Lemahieu, and R. Van De Walle, "Hex-spline: a novel family for hexagonal lattices," *IEEE Trans. Image Processing*, vol. 13, no. 6, pp. 758–772, June 2004.
- [3] M. Unser, "Splines: A perfect fit for signal and image processing," *IEEE Signal Processing Mag.*, vol. 16, no. 6, pp. 22–38, Nov. 1999.
- [4] R. M. Mersereau, "The processing of hexagonally sampled two-dimensional signals," *Proc. IEEE*, vol. 67, no. 6, pp. 930–949, June 1979.
- [5] D. P. Petersen and D. Middleton, "Sampling and reconstruction of wavenumber-limited functions in  $N$ -dimensional Euclidean spaces," *Information and Control*, vol. 5, pp. 279–323, 1962.
- [6] C. de Boor, K. Höllig, and S. Riemenschneider, *Box Splines*. Berlin: Springer-Verlag, 1993, vol. Applied Mathematical Sciences, vol. 98.
- [7] R. DeVore and A. Ron, "Developing a computation-friendly mathematical foundation for spline functions," *SIAM News*, vol. 38, no. 4, May 2005.
- [8] S. Malassiotis and M. G. Strintzis, "Optimal biorthogonal wavelet decomposition of wire-frame meshes using box splines, and its application to the hierarchical coding of 3-D surfaces," *IEEE Trans. Image Processing*, vol. 8, no. 1, pp. 41–57, Jan. 1999.
- [9] H. Prautzsch and W. Boehm, "Box splines," in *Handbook of Computer Aided Geometric Design*. Berlin: Springer, 2001.
- [10] E. Cohen, T. Lyche, and R. Riesenfeld, "Discrete box splines and refinement algorithms," *Comput. Aided Geom. Design*, vol. 1, pp. 131–141, 1984.
- [11] W. Dahmen and C. A. Michelli, "Subdivision algorithms for the generation of box-spline surfaces," *Comput. Aided Geom. Design*, vol. 1, pp. 115–129, 1984.
- [12] —, "Line average algorithm: a method for the computer generation of smooth surfaces," *Comput. Aided Geom. Design*, vol. 2, pp. 77–85, 1985.
- [13] C. K. Chui and M.-J. Lai, "Algorithms for generating B-nets and graphically displaying spline surfaces on three- and four-directional meshes," *Comput. Aided Geom. Design*, vol. 8, no. 6, pp. 479–493, 1991.
- [14] M.-J. Lai, "Fortran subroutines for B-nets of box splines on three and four directional meshes," *Numerical Algorithms*, vol. 2, pp. 33–38, 1992.
- [15] C. D. Boor, "On the evaluation of box splines," *Numerical Algorithms*, vol. 5, pp. 5–23, Mar. 1993.
- [16] L. Kobbelt, "Stable evaluation of box-splines," *Numerical Algorithms*, vol. 14, no. 4, pp. 377–382, 1997.